Speeding up critical system dynamics through optimized evolution

Tommaso Caneva,[1,2] Tommaso Calarco,[2] Rosario Fazio,[3] Giuseppe E. Santoro,[1,4,5] and Simone Montangero[2]

[1]*International School for Advanced Studies (SISSA), Via Beirut 2-4, I-34014 Trieste, Italy*

[2]*Institut für Quanteninformationsverarbeitung, Universität Ulm, D-89069 Ulm, Germany*

[3]*NEST, Scuola Normale Superiore & Istituto di Nanoscienze-CNR, Piazza dei Cavalieri 7, I-56126 Pisa, Italy*

[4]*CNR-INFM Democritos National Simulation Center, Via Beirut 2-4, I-34014 Trieste, Italy*

[5]*International Centre for Theoretical Physics (ICTP), P.O. Box 586, I-34014 Trieste, Italy*

The number of defects which are generated upon crossing a quantum phase transition can be minimized by choosing properly designed time-dependent pulses. In this work we determine what are the ultimate limits of this optimization. We discuss under which conditions the production of defects across the phase transition is vanishing small. Furthermore we show that the minimum time required to enter this regime is $T \sim \pi/\Delta$, where Δ is the minimum spectral gap, unveiling an intimate connection between an optimized unitary dynamics and the intrinsic measure of the Hilbert space for pure states. Surprisingly, the dynamics is nonadiabatic; this result can be understood by assuming a simple two-level dynamics for the many-body system. Finally we classify the possible dynamical regimes in terms of the action $s = T\Delta$.

PACS number(s): 03.67.−a, 64.70.Tg

I. INTRODUCTION

The rapid progress in the experimental realization and manipulation of quantum systems [1] is opening the rich and intriguing perspective of the exploitation of quantum physics to realize quantum technologies like quantum simulators [2] and quantum computers [3,4]. These achievements pave the way to the simulation of condensed matter systems giving the possibility of studying different states of matter in controlled experiments [5]. Despite the impressive results obtained so far, this is a formidable technological and theoretical challenge due to the complexity of the systems in analysis and the experimental requirements. Indeed, the level of control needed over the quantum system is unprecedented: one should be able to prepare a system in a desired initial state, perform the desired evolution, and finally measure the state in a very precise way. Moreover, the whole experiment should be performed faster than the system decoherence time that eventually will destroy any quantum information capability.

Quantum optimal control (OC) theory, the study of optimization strategies to improve the outcome of a quantum process, can be an extremely powerful tool to cope with these issues [6–10]. It allows one not only to optimize the desired experiment outcome but also to speed up the process itself. Traditionally employed in atomic and molecular physics [11,12], OC has been recently applied with success to the optimization of the dynamics of many-body systems [13–15], allowing one to achieve the ultimate bound imposed by quantum mechanics, the so-called *quantum speed limit* (QSL) [16]. Indeed as intuitively suggested by the time-energy uncertainty principle, the time required by a state to reach another distinguishable state has to be longer than the inverse of its energy fluctuations [17]. This implies that a quantum system cannot evolve at an arbitrary speed in its Hilbert space, but a minimum time is required to perform a transformation between orthogonal states [18–22]. For time-independent Hamiltonians this bound has been exactly determined [16];

the QSL has been formally generalized also to time-dependent Hamiltonians, but so far has been computed only in a few simple cases [13,23–26].

A still unexplored, although relevant, question is how the dynamical crossing of a quantum phase transition (QPT) affects this fundamental bound. QPTs indeed represent a dramatic change in the low-energy sector of a quantum system and their presence strongly influence its dynamics. The study of the dynamical crossing of phase transitions was initially considered in cosmology to investigate the formation of the universe [27]. More recently with the development of the quantum annealing [28] and adiabatic quantum computation [4], a renewed interest has been devoted to the subject in condensed matter and quantum information [29–32]. Here we investigate for the first time the QSL of the dynamics of a first-order QPT in the adiabatic version of Grover's search algorithm (GSA) [33,34] and of a second-order QPT [35] in the Lipkin-Meshkov-Glick (LMG) model. Specifically we consider the problem of converting the ground state on one side of the critical point into the ground state on the opposite side in the fastest and most accurate way by selecting an optimal time-dependence of the control field. We emphasize here that the evolution induced by the optimized field is nonadiabatic, as shown in Fig. 1, where the scenario is reproduced for the LMG model and an adiabatic and an optimal evolution are compared: an adiabatic strategy (orange continuous line along bottom axis) turns out to be effective only for a very large total evolution time T (namely, $T \gg \hbar\Delta^{-1}$, with Δ being the minimum spectral gap, as required by the adiabatic theorem [36]). When the total time is reduced, as realistically required in experiments in order to preserve the phase coherence, adiabaticity fails, leading to an excited state far from the target (red dot-dashed line). However, relaxing the constraint of adiabaticity and allowing a more general nonadiabatic evolution, with OC it is possible to reach the desired goal with a fast dynamics (green dashed line). Quite surprisingly our study
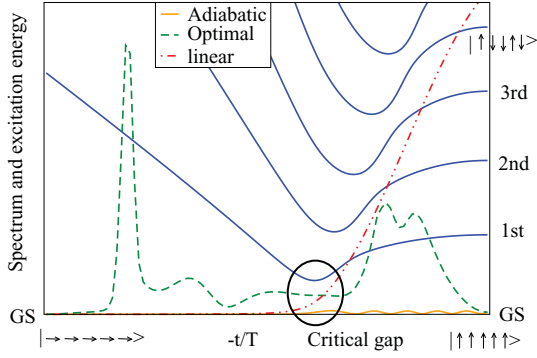
FIG. 1. (Color online) Instantaneous excitation energy in the LMG model for an optimized (green dashed line, total time $T \sim T_{QSL}$), a non optimized (red dot-dashed line, $T \sim T_{QSL}$) and a linear adiabatic process (orange continuous line, $T \gg T_{QSL}$). Continuous (blue) lines represents the lowest energy levels as a function of the driving field $\Gamma = -t/T$.

shows that the outcome of the dynamical process optimization for the many-body systems analyzed is independent from the specific model and analogous to that of a two-level system, as sketched through the good rescaling of the data in Fig. 2. We interpret this result as the natural manifestation of the intrinsic metric of the Hilbert space for pure states [23,37], as discussed in Sec. III A. Furthermore, studying the QSL as a function of the system size, we show that the speedup obtained by the adiabatic GSA [33,38] can be reproduced and extended to other models with optimized, nonadiabatic evolutions. Finally, we introduce the action $s = T \Delta$ as a parameter to characterize the evolution of a quantum system and we find that the QSL identifies a new dynamical regime, as discussed in Sec. III B and summarized in Fig. 5.

II. MODELS AND OPTIMIZATION

We study two paradigmatic critical systems, the adiabatic GSA [33] and the LMG model [39] and we compare them with the Landau-Zener (LZ) model to better understand the physics of the process.
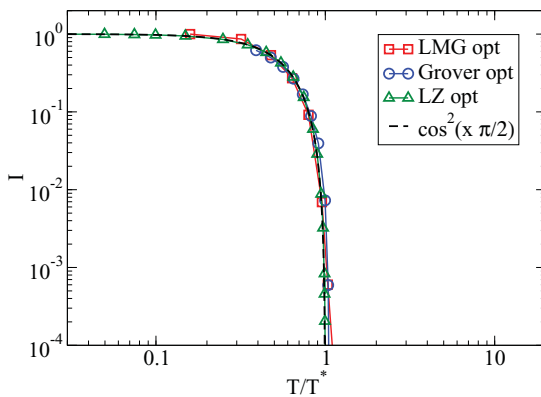

FIG. 2. (Color online) Infidelity I as a function of the adimensional scaling variable T/T^* for the LMG model (red squares), the Grover model (blue circles), and the LZ model (green triangles). Data correspond to half of the maximum size analyzed ($N = 64$).

The GSA Hamiltonian is given by

$$H^{\mathrm{GSA}} = [1 - \Gamma(t)](I - |\psi_i\rangle\langle|\psi_i|) + \Gamma(t)(I - |\psi_G\rangle\langle|\psi_G|), \quad (1)$$

where the initial state is an equal superposition of all N basis states $|i\rangle$, i.e., $|\psi_i\rangle = (\sum_i^N |i\rangle)/\sqrt{N}$ and the final target is the specific marked state we want to extract from the database (in our simulations $|\psi_G\rangle = |10, \ldots, 0\rangle$ without loss of generality). The system undergoes a first-order QPT at a critical value of the transverse field $\Gamma_c = 0.5$ (from now on we set $\hbar = 1$). The gap between the ground state and first excited state closes polynomially with the size at the critical point: $\Delta_{\mathrm{GSA}} \sim N^{-1/2}$.

The LMG Hamiltonian instead is written as

$$H^{\mathrm{LMG}} = -\sum_{i<j}^N J_{ij}\sigma_i^x\sigma_j^x - \Gamma(t)\sum_i^N \sigma_i^z, \quad (2)$$

where N is the number of spins, σ_i^α's ($\alpha = x, y, z$) are the Pauli matrices on the ith site, and $J_{ij} = 1/N$ (infinite range interaction). The system undergoes a second-order QPT from a quantum paramagnet to a quantum ferromagnet at a critical value of the transverse field $|\Gamma_c| = 1$. The gap between the ground state and first excited state closes polynomially with the size at the critical point: $\Delta_{\mathrm{LMG}} \sim N^{-1/3}$. We chose as the initial state the ground state (GS) at $\Gamma_i \gg 1$, i.e., the state in which all the spins are polarized along the positive z axis (paramagnetic phase). As the target state we chose the GS at $\Gamma = 0$.

Finally the LZ Hamiltonian that we use as a reference model is

$$H^{\mathrm{LZ}} = \Gamma(t)\sigma_z + \omega\sigma_x, \quad (3)$$

where the off-diagonal terms give the amplitude of the minimum gap $\Delta_{\mathrm{LZ}} = 2\omega$ at the anticrossing point $\Gamma = 0$, here assumed to be at $t = 0$ [29,40]. In this case the initial state is the GS for $\Gamma(-T/2) = -\Gamma_0$ and the target is the GS for $\Gamma(T/2) = \Gamma_0$, that is—in this effective model—to transform the initial GS into the initial excited state in the optimal and fastest way. The systems analyzed are summarized in the left side of Table I.

For all the models considered our goal is to find the optimal driving control field $\Gamma(t)$ to transform the initial state in the goal state in a given total time T. At the limit when the gap closes (the thermodynamical limit for GSA and LMG) adiabatic dynamics is forbidden in finite time due to the adiabatic condition $T \gg \Delta^{-1}$ [36]: however, for finite-size systems, an adiabatic strategy might be successful. Here we relax the adiabaticity condition, exploring a different regime of fast nonadiabatic transformations. Given the total evolution time T, we use optimal control through the Krotov's algorithm to find the optimal control field $\Gamma(t)$ to minimize the infidelity $I(T) = 1 - |\langle\psi_G|\psi(T)\rangle|^2$ at the end of the evolution, i.e., the discrepancy between the final and the goal state [6]. The determination of $\Gamma_{\mathrm{opt}}(t)$ can be recast in a minimization problem subject to constraints determined by looking for the stationary points of a functional $\mathcal{L}[\psi, \dot{\psi}, \chi, \Gamma]$ in which the auxiliary states $|\chi(T)\rangle = |\psi_G\rangle\langle\psi_G|\psi(T)\rangle$ play the role of a continuous set of Lagrange multipliers to impose the

TABLE I. Hamiltonian models and predicted scalings in the LZ approximation for the linear and optimal quenches. They should be compared with the results of Fig. 4. The functions $f_i(I)$ diverge for the infidelity $I \to 0$.

Model	H	$\lvert\psi_i\rangle$	$\lvert\psi_G\rangle$	Δ	s^*_{Lin}	s^*_{Opt}
GSA	$[1 - \Gamma(t)](\mathbf{1} - \lvert\psi_i\rangle\langle\lvert\psi_i\rvert) + \Gamma(t)(\mathbf{1} - \lvert\psi_G\rangle\langle\lvert\psi_G\rvert)$	$\sum_i^N \lvert i\rangle/\sqrt{N}$	$\lvert 10, \ldots, 0\rangle$	$N^{-1/2}$	$f_1(I)N^{1/2}$	$\xrightarrow{N \gg 1} \pi$
LMG	$-(N^{-1})\sum_{i<j}^N \sigma_i^x\sigma_j^x - \Gamma(t)\sum_i^N \sigma_i^z$	$\lvert\uparrow\cdots\uparrow\rangle_z$	$\lvert\leftarrow\cdots\leftarrow\rangle_x, \lvert\rightarrow\cdots\rightarrow\rangle_x$	$N^{-1/3}$	$f_2(I)N^{1/3}$	π
LZ	$\Gamma(t)\sigma^z + \omega\sigma^x$	$\lvert\uparrow\rangle_z$	$\lvert\downarrow\rangle_z$	Δ	$[-4\ln(I)/\pi]\Delta^{-1}$	π

fulfillment of the Schrödinger equation at each time during the dynamics, as described in detail in Refs. [6,9,12].

III. RESULTS

A. Hilbert space metric and optimization

Previous studies [13] have revealed that only when the total evolution time exceeds a certain threshold, by iterating the algorithm, it is possible to reduce arbitrarily the value of the final infidelity I. In order to identify such a threshold, we fix a target value of the infidelity $I^* \sim 10^{-3}$ and we determine the minimum total evolution time T^* for which it is possible to satisfy our goal. In Fig. 2 we show the value of the infidelity for the optimized process as a function of the rescaled time T/T^* for different models. The first observation is the presence of a sharp threshold; thus, T^* can be considered a reliable estimate of the QSL for the process considered. The second striking feature is the rescaling of the data onto the function $I = \cos^2(T/T^*)$. We interpret this general behavior as a manifestation of the Fubini-Study metric [23,37] in the Hilbert space. The presence of such a metric for pure states can be demonstrated following two independent approaches: Wootters in Ref. [37] obtained it just from statistical considerations; Anandan and Aharonov instead in Ref. [23] derived it by generalizing the concept of the geometrical Berry's phase to generic nonadiabatic evolutions. According to the Fubini-Study metric the distance separating two arbitrary pure states is given by the angle between the corresponding rays, $\theta_G/2 = \arccos\lvert\langle\psi_i\lvert\psi_G\rangle\rvert$. For orthogonal states this distance is maximal and given by $\theta_G = \pi$. The shortest path connecting the states $\lvert\psi_i\rangle$ and $\lvert\psi_G\rangle$ is then represented by a geodesic in the ray subspace. We can indicate

a ray evolving along such a geodesic with $\lvert\psi_\theta\rangle$, where $0 < \theta < \theta_G$, so that $\lvert\psi_0\rangle = \lvert\psi_i\rangle$ and $\lvert\psi_{\theta_G}\rangle = \lvert\psi_G\rangle$, as sketched in Fig. 3. For such a ray it turns out $\lvert\langle\psi_\theta\lvert\psi_G\rangle\rvert^2 = \cos^2[(\theta_G - \theta)/2]$ or, for the infidelity, $I_\theta = \sin^2[(\theta_G - \theta)/2]$. Numerically it can be verified that for states on opposite sides of a QPT $\theta_G \simeq \pi$; substituting this value in the expression of the infidelity, we obtain $I_\theta \simeq \cos^2(\theta/2)$. Making the identification $\theta = \pi T/T^*$ this last formula is in perfect agreement with the data of Fig. 2 and with the results for a two-level system in Ref. [12]. An optimized evolution then can be interpreted as a uniform motion along a geodesic with speed π/T^*.

B. Dynamical regime classification

In order to establish a classification of dynamical regimes and to understand the speedup that optimized evolutions gain with respect to nonoptimized pulses, we introduce the action $s = T\Delta$, obtained through the product of the total evolution time with the minimum spectral gap. Notice this is a quite natural way to characterize a dynamical process: $s \gg 1$ corresponds to a slow evolution, for which in principle an adiabatic dynamics could be achieved; $s \leqslant 1$ instead characterizes a fast evolution, for which adiabaticity is strictly forbidden. In Fig. 4 the data for optimal driving fields (open symbols) are compared with data obtained with a linear time dependence (solid symbols) $\Gamma(t) = t/T$ for the GSA, the LMG, and the LZ models. We report the product $s^* = T^*\Delta$ as a function of the size N, Δ being the minimum spectral gap and T^* the minimal time required to reach an infidelity $I^* \sim 10^{-3}$.

FIG. 4. (Color online) The action $s^* = T^*\Delta$ as a function of the size N (for the LZ model we define an effective size $N = \Delta^{-1}$), where Δ is the minimum spectral gap and T^* the time required to reach an infidelity $I^* \sim 10^{-3}$ for the linear (solid symbols) and optimized (open symbols) driving field for the LMG model (red squares), the Grover model (blue circles), and the LZ model (green triangles).
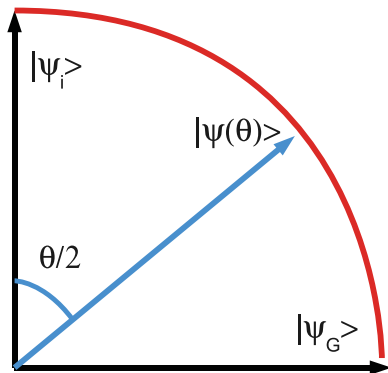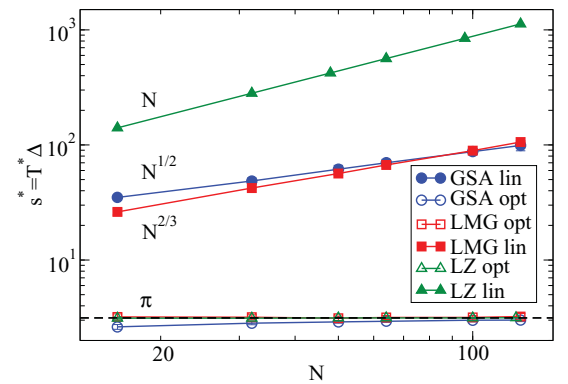

FIG. 3. (Color online) Schematic representation of the ray $\lvert\psi_\theta\rangle$ evolving along the geodesic connecting the initial state $\lvert\psi_i\rangle$ and the target $\lvert\psi_G\rangle$.

As can be clearly seen in Fig. 4, a linear time-dependent $\Gamma(t)$ results in an action s^* increasing with the system size, implying that $T^* \sim \Delta^{-\alpha}$ with $\alpha > 1$ (solid symbols). On the contrary, the action s^* remains below the value π after the optimization (open symbols). Notice that the optimal action is reduced by 1 to 2 orders of magnitude in Fig. 4, but in general $s^*_{\text{Opt}} \sim \pi$ and $s^*_{\text{Lin}} \to \infty$ for $I^* \to 0$. A simple interpretation of the scalings reported in the picture can be understood as follows. For a linear quench, in a first approximation, we can assume that the main contribution to the infidelity comes only from the first excited state [29], and the Landau-Zener formula [40] can be used to give an estimate of the excitation probability, i.e., the infidelity, $\mathcal{I} = \exp(-\beta \Delta^2 T)$, with $\beta = \text{const}$, so that by fixing an arbitrary (but small) value for the infidelity $\mathcal{I}^*$, we have $T^* \sim \Delta^{-2}$ or $s^* \sim \Delta^{-1}$. By inserting the gap dependence on the size, the scalings reported in Table I are obtained for the models considered in this work: they are in almost perfect agreement with the numerical data reported in Fig. 4, where s^*_{Lin} is increasing with the size. The only discrepancy is the scaling of the linear LMG model due to the fact that the simple linear LZ approximation fails. Indeed, here we have that $\beta = \beta(N) \sim N^{-1/3}$, resulting in $T^* \sim \Delta^{-3}$, that is, $s^*_{\text{Lin}} = N^{2/3}$. For the optimized process instead, the optimal value $s^*_{\text{Opt}} = \pi$ corresponds to a Rabi oscillation between the initial state and the target state at a frequency $\omega_R = \Delta/2$, as clearly shown in Fig. 2; or in other words, according to our geometrical interpretation, the optimal evolution can be seen as a motion along a geodesic connecting the initial state and the target state at a constant speed proportional to Δ [25]; an intuitive explanation is provided in the Appendix. As shown in Fig. 4, the speedup we have obtained in our analysis is analogous to the speedup reached through the Grover's quantum adiabatic algorithm [33], from a quadratic to a linear dependence on gap of the evolution time T^*. In the case of the LMG model the gain is stronger, from a cubic to a linear dependence, outlining the fact that the limit of the optimization is set by a constant value of the action $s^* = T^*\Delta$. As a last remark, from the previous discussion it can be argued that optimized evolutions achieve a substantial speedup only when the minimum gap closes polynomially with the size; in the case of an exponential closure, even an optimized process leads to a total evolution time exponentially diverging with N [41–45].

We summarize the possible regimes of a quantum evolution in Fig. 5, where the final infidelity and the time scale as a function of the action s are shown. An optimized process
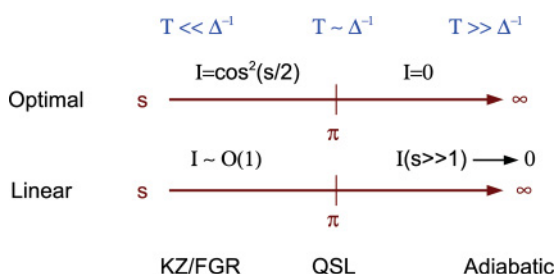

FIG. 5. (Color online) The different dynamical regimes as a function of the action s.

is characterized by $I = \cos^2(s/2)$ for $s \leqslant \pi$ and $I = 0$ for $s > \pi$. For a linear nonoptimized pulse, $s \leqslant \pi$ indicates a fast evolution with high defect production [$I \sim O(1)$] accurately estimated by the Kibble-Zurek (KZ) theory [29] or the Fermi golden rule (FGR) approximation [30]. On the contrary, for $s \gg \pi$ adiabaticity can be achieved and the infidelity is asymptotically vanishing. The QSL then clearly identifies the threshold between fast and adiabatic evolutions.

IV. CONCLUSION

In conclusion, we estimated the time required by an optimized, nonadiabatic process to drive the ground state of a many-body system across a quantum phase transition. The behavior of the systems analyzed was revealed to be surprisingly similar to that of a simple two-level system; we explained the phenomenon through the connection with the intrinsic geometry of the Hilbert space for pure state, interpreting the optimized process as a uniform motion along the geodesic connecting the initial and target states, as summarized in Fig. 2. This result is of particular relevance because it establishes a direct link between the QSL and Fisher information [22] in the general setup of an evolution driven by a time-dependent Hamiltonian. We demonstrated that the QSL for the dynamical processes analyzed scales as the inverse of the critical gap, significantly improving the result obtained with a nonoptimized evolution. Such a speedup is a general feature and can be interpreted as the extension of the Grover's algorithm speedup to the models considered. Finally, introducing the action s, we provided a classification of the possible QPT dynamics. We mention that the understanding of these optimal processes and of the fundamental time scales might be used to develop new and more efficient optimization strategies also in quantum state preparation.

APPENDIX

In this appendix we provide an intuitive explanation for the scaling obtained in Sec. III B. The numerical results suggest that the optimized process is equivalent to perform a rotation of the initial state into the target at a constant angular speed $\omega = \Delta/2$, where $\Delta = f(N)$ is the critical gap of the finite-size many-body system in analysis. In a first approximation we can recast the full many-body problem into a two-level effective model, described with a LZ-like Hamiltonian $H^{\text{LZ}}[\Gamma(t)]$, where the spin-up and spin-down states play, respectively, the role of the full many-body initial and target states and the tunability of the diagonal element $\Gamma(t)$ mimics the possibility of selecting the instantaneous rotational axis. Considering Fig. 6, intuitively one can expect that the initial state does
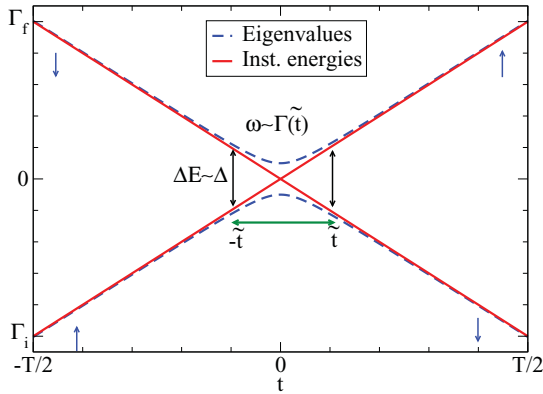
FIG. 6. (Color online) Instantaneous eigenvalues (blue dashed lines) and uncoupled energies of the spin-up, spin-down configurations (red continuous lines) of the LZ model for a linear quench, $\Gamma \sim t/T$. The time $\tilde{t}$ represents the boundary between Region I with high transformation rate ($|t| \leqslant \tilde{t}$) and Region II where the system is in the instantaneous ground state ($|t| \geqslant \tilde{t}$).

not change significantly while its energy is much larger than the off-diagonal matrix elements, while vice versa, an efficient

population transfer occurs when $\Gamma(t) \lesssim \omega$. Therefore the total evolution can be approximated in two distinct regimes: a first one for $|\Gamma(t)| \gg \omega$ in which $H^{\mathrm{LZ}} \sim \Gamma(t)\sigma_z$ and the initial state corresponds to the instantaneous GS, and a second regime for $|\Gamma(t)| \ll \omega$ where the two levels are highly coupled and $H^{\mathrm{LZ}} \sim \omega\sigma_x$. The time $\tilde{t}$ marking the boundary between the two regimes is implicitly determined by the condition

$$\Gamma(\tilde{t}) \sim \omega, \qquad (A1)$$

as shown in Fig. 6. Under this approximation, the optimization problem is now easily solved. It is indeed known that the fastest possible transition between two orthogonal states with a fixed overlap ω is obtained through a Rabi oscillation, i.e., by applying $H = \omega\sigma_x$ for a time $T_c = \pi/2\omega$ [3,23]. The complete rotation is then possible if the condition $T_c \sim \tilde{t}$ holds, where $\tilde{t}$ is obtained solving Eq. (A1). A linear time dependence of the field, $\Gamma(t) = t/T$, gives $\tilde{t} \sim \omega T$, that is, $T \sim \omega^{-2} \sim \Delta^{-2}$, implying $s_{\mathrm{Lin}}^* \sim \Delta^{-1}$. The optimization of the time dependence of $\Gamma(t)$ corresponds to the extension of the region of high transition rate, i.e., to the increase of $\tilde{t}$; the best possible result is clearly $\tilde{t} \sim T$, that is, the transformation is effective during the whole evolution. Finally setting this condition, we obtain $T \sim \pi/2\omega \sim \pi\Delta^{-1}$ and $s_{\mathrm{Opt}}^* \sim \pi$.

[1] I. Bloch, J. Dalibard, and W. Zwerger, Rev. Mod. Phys. **80**, 885 (2008).
[2] R. Feynman, Int. J. Theor. Phys. **21**, 467 (1982).
[3] S. Lloyd, Nature (London) **406**, 1047 (2000).
[4] E. Farhi, J. Goldstone, S. Gutmann, J. Lapan, A. Lundgren, and D. Preda, Science **292**, 472 (2001).
[5] K. Baumann, C. Guerlin, F. Brennecke, and T. Esslinger, Nature (London) **464**, 1301 (2010).
[6] V. F. Krotov, *Global Methods in Optimal Control Theory* (Dekker, New York, 1996).
[7] I. R. Sola, J. Santamaria, and D. J. Tannor, J. Phys. Chem. A **102**, 4301 (1998).
[8] N. Khaneja, T. Reiss, C. Kehlet, T. Schulte-Herbruggen, and S. G. Glaser, J. Magn. Res. **172**, 296 (2005).
[9] S. Montangero, T. Calarco, and R. Fazio, Phys. Rev. Lett. **99**, 170501 (2007).
[10] C. Brif, R. Chakrabarti, and H. Rabitz, New J. Phys. **12**, 075008 (2010).
[11] A. P. Peirce, M. A. Dahleh, and H. Rabitz, Phys. Rev. A **37**, 4950 (1988).
[12] T. Calarco, U. Dorner, P. Julienne, C. J. Williams, and P. Zoller, Phys. Rev. A **70**, 012306 (2004).
[13] T. Caneva, M. Murphy, T. Calarco, R. Fazio, S. Montangero, V. Giovannetti, and G. E. Santoro, Phys. Rev. Lett. **103**, 240501 (2009).
[14] P. Doria, T. Calarco, and S. Montangero, Phys. Rev. Lett. **106**, 190501 (2011).
[15] A. Rahmani and C. Chamon, e-print arXiv:1011.3061.
[16] V. Giovannetti, S. Lloyd, and L. Maccone, Phys. Rev. A **67**, 052109 (2003).
[17] Y. Aharonov and D. Bohm, Phys. Rev. **122**, 1649 (1961).
[18] K. Battacharyya, J. Phys. A **16**, 2993 (1983).
[19] N. Margolus and L. B. Levitin, Physica D **120**, 188 (1998).
[20] L. B. Levitin and T. Toffoli, Phys. Rev. Lett. **103**, 160502 (2009).
[21] A. Smerzi, e-print arXiv:1002.2760.

[22] P. J. Jones and P. Kok, Phys. Rev. A **82**, 022107 (2010).
[23] J. Anandan and Y. Aharonov, Phys. Rev. Lett. **65**, 1697 (1990).
[24] P. Pfeifer, Phys. Rev. Lett. **70**, 3365 (1993).
[25] A. Carlini, A. Hosoya, T. Koike, and Y. Okudaira, Phys. Rev. Lett. **96**, 060503 (2006).
[26] A. T. Rezakhani, W.-J. Kuo, A. Hamma, D. A. Lidar, and P. Zanardi, Phys. Rev. Lett. **103**, 080502 (2009).
[27] W. H. Zurek, Nature (London) **317**, 505 (1985).
[28] J. Brooke, D. Bitko, T. F. Rosenbaum, and G. Aeppli, Science **284**, 779 (1999).
[29] W. H. Zurek, U. Dorner, and P. Zoller, Phys. Rev. Lett. **95**, 105701 (2005).
[30] A. Polkovnikov and V. Gritsev, Nat. Phys. **4**, 477 (2008).
[31] J. Dziarmaga, Adv. Phys. **59**, 1063 (2010).
[32] A. Polkovnikov, K. Sengupta, A. Silva, and M. Vengalattore, e-print arXiv:1007.5331.
[33] J. Roland and N. J. Cerf, Phys. Rev. A **65**, 042308 (2002).
[34] A. T. Rezakhani, A. K. Pimachev, and D. A. Lidar, Phys. Rev. A **82**, 052305 (2010).
[35] S. Sachdev, *Quantum Phase Transition* (Cambridge University Press, Cambridge, UK, 1999).
[36] A. Messiah, *Quantum Mechanics*, Vol. 2 (North-Holland, Amsterdam, 1962).
[37] W. K. Wootters, Phys. Rev. D **23**, 357 (1981).
[38] L. K. Grover, Phys. Rev. Lett. **79**, 325 (1997).
[39] R. Botet and R. Jullien, Phys. Rev. B **28**, 3955 (1983).
[40] C. Zener, Proc. R. Soc. A **137**, 696 (1932).
[41] J. Dziarmaga, Phys. Rev. B **74**, 064416 (2006).
[42] T. Caneva, R. Fazio, and G. E. Santoro, Phys. Rev. B **76**, 144427 (2007).
[43] M. H. S. Amin and V. Choi, Phys. Rev. A **80**, 062326 (2009).
[44] B. Altshuler, H. Krovi, and J. Roland, PNAS **107**, 12446 (2010).
[45] A. P. Young, S. Knysh, and V. N. Smelyanskiy, Phys. Rev. Lett. **104**, 020502 (2010).